Crystal Structure, Sensitiveness and Theoretical Explosive Performance of Xylitol Pentanitrate (XPN)

Kelly-Anne S. Stark,[a] Jason F. Alvino,[b] K. Paul Kirkbride,[a] Christopher J. Sumby,[b] Gregory F Metha,[b] Claire E. Lenehan,[a] Mark Fitzgerald,*[c] Craig Wall,[c] Mark Mitchell,[c] and Chad Prior[c]

Abstract: Xylitol pentanitrate (XPN) is a little-studied nitrate ester of similar molecular structure to the military energetic materials pentaerythritol tetranitrate (PETN) and nitroglycerin (NG). XPN was crystallised from a mixture of ethanol and water by slow evaporation and studied by single crystal X-ray diffraction. XPN crystallises in the centrosymmetric monoclinic space group P2$_1$/n, with a calculated density of 1.852 g cm^{-3}. Sensitiveness analysis of the energetic material revealed it to be a primary explosive, sig-

nificantly more sensitive than PETN to friction and impact. The calculated heat of formation of XPN, -500.48 kJ mol^{-1}, and the density were exploited utilising the Cheetah 7.0 suite of programs to predict explosive performance parameters. The theoretical explosive performance of XPN was comparable to the calculated explosive parameters of erythritol tetranitrate (ETN), PETN and cyclotrimethylene trinitramine (RDX).

Keywords: Nitrate ester · Xylitol pentanitrate · explosive performance · crystal structure · sensitivity

1 Introduction

Nitroglycerin (NG) and pentaerythritol tetranitrate (PETN) are nitrate esters which are in common usage by military forces worldwide. Erythritol tetranitrate (ETN) has been exhaustively investigated for potential use by conventional armed forces, but has yet to find legitimate applications due to poor chemical stability. In contrast, xylitol pentanitrate (XPN), a nitrate ester similar in structure to NG, PETN and ETN (Figure 1), only appears sparingly in the scientific literature.

XPN was first isolated as a crystalline solid in 1960 [1], with a refined synthetic procedure reported three years later [2]. The nitrate, described as a powerful explosive, was formed by the direct nitration of xylitol in a mixture of fuming nitric acid and acetic anhydride, with the structure confirmed by nitrogen content analysis, infra-red spectroscopy and the near-quantitative catalytic hydrogenation to the parent alcohol.

In 1971 a pharmacological and biochemical evaluation of organic nitrates found XPN was a poor vasodilator compared to NG and PETN [3].

Nearly forty years later, Šarlauskas *et al.* reported the synthesis, electrochemistry and cytotoxicity of a series of nitrate esters and nitramines, including XPN [4,5]. The authors alluded to a synthetic methodology involving the treatment of xylitol with dinitrogen pentoxide in dichloromethane and subsequent characterisation of the isolated product by TLC, IR and NMR spectroscopy; however, neither the detailed synthetic procedure nor the characterisation data were published.

Concomitantly, Wang *et al.* published a theoretical study predicting the spectral, physical, thermodynamic and energetic properties of XPN, and other related compounds, and was suggested as a possible candidate for use in solid rocket propellant formulations [6]. Molecular structures predicted by density functional theory at the B3LYP/6-31G* level of theory were utilised to predict theoretical densities. These results were combined with heats of formation derived from the semiempirical molecular orbital PM3 method to predict detonation velocity and detonation pressure using modified Kamlet-Jacobs equations [7,8].

Qi-Long et al. reported the thermal stability and decomposition mechanism functions of ten nitrate esters, including XPN, by means of non-isothermal Thermal Gravimetric (TG) and Differential Scanning Calorimetry (DSC) techniques [9,10]. Comparison of mean activation energies indicated that all species shared common decomposition pathways, but analyses of critical temperatures of thermal decomposition revealed XPN as one of the least stable nitrate esters. Other than the abovementioned analyses, no structural

[a] *K.-A. S. Stark, K. P. Kirkbride, C. E. Lenehan*
Flinders University, South Australia, Sturt Road, Bedford Park, South Australia, 5042, Australia

[b] *J. F. Alvino, C. J. Sumby, G. F Metha*
Department of Chemistry, The University of Adelaide, South Australia, 5005, Australia

[c] *M. Fitzgerald, C. Wall, M. Mitchell, C. Prior*
Weapons and Combat Systems Division, Defence Science and Technology Group, West Avenue, Edinburgh, South Australia, 5111, Australia
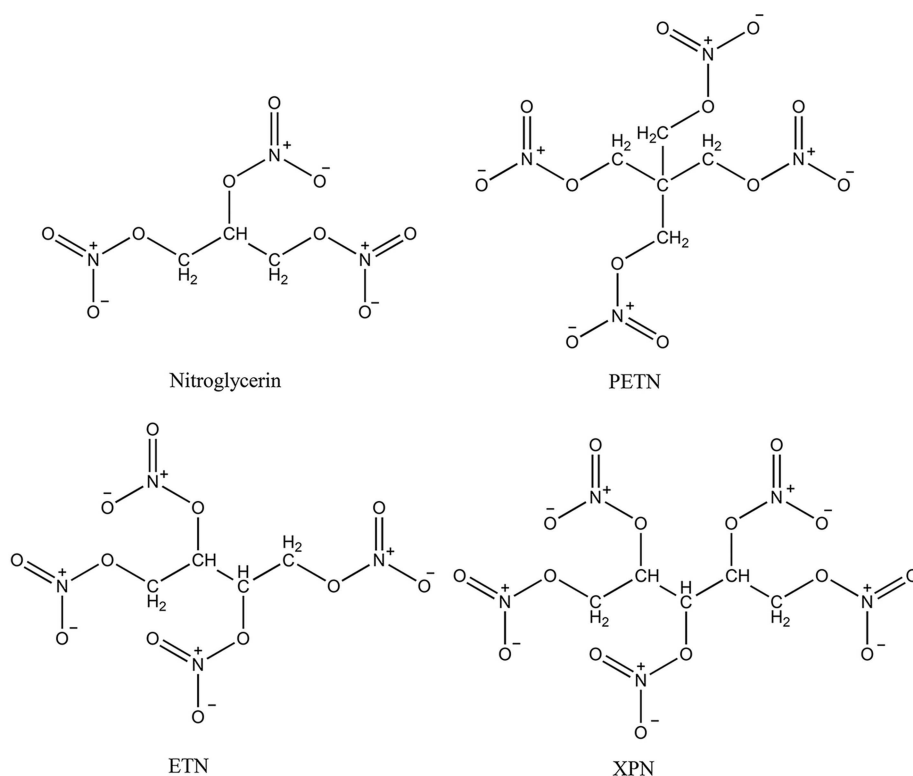**e-mail: mark.fitzgerald2@dst.defence.gov.au*

Figure 1. Simple molecular structures of NG, PETN, ETN and XPN.

characterisation data were provided and it is unclear if XPN was isolated as a crystalline solid.

Herein, the single crystal X-ray diffraction (SCXRD) structure and sensitiveness data for XPN are reported for the first time. The molecular structure from SCXRD was utilised as the starting geometry for CBS-4M quantum chemical calculations to accurately derive heat of formation [11,12]. The density of XPN, derived from crystallographic analysis, and the calculated heat of formation were subsequently exploited using the thermochemical computer code Cheetah [13] to predict explosive performance. This revealed the theoretical explosive performance of XPN is comparable to some military high explosives.

2 Experimental Section

2.1 Reagents

Xylitol, 98% sulfuric acid, acetic anhydride, toluene and ethanol (Sigma-Aldrich, St Louis, USA) were used as received. Red fuming nitric acid (Sigma-Aldrich, St Louis, USA) was distilled before use.

2.2 Synthetic Procedure

Caution: XPN is a sensitive primary explosive and as such should only be synthesised in minimal quantities by experienced and appropriately trained chemists, in purpose-built explosives laboratories.

XPN was synthesized using a literature procedure [2].

2.3 Single Crystal X-ray Diffraction

A single XPN crystal was mounted under paratone-N oil on a nylon loop, and X-ray diffraction data were collected at 150(2) K with Mo Kα radiation ($\lambda = 0.7107$ Å) on an Oxford Diffraction X-calibur small molecule diffractometer [14]. The data set was corrected for absorption and the structure solved by direct methods using SHELXS-2014 and refined by full matrix least-squares on F^2 by SHELXL-2014, interfaced through the program X-Seed [15–17]. In general, all non-hydrogen atoms were refined anisotropically, and hydrogen atoms were included as invariants at geometrically estimated positions. CCDC number 1869403 contains the supplementary crystallographic data for this paper. These data can be obtained free of charge from The Cambridge Crystallographic Data Centre via www.ccdc.cam.ac.uk/data_request/cif.

Crystal data for XPN. $C_5H_7N_5O_{10}$, F.w. 377.16, monoclinic, $P2_1/n$, *a* 8.0945(3), *b* 15.9392(6), *c* 10.4903(5) Å, β 91.684(3)°, *V* 1352.87(10) Å^3, $Z = 4$, $D_{calc} = 1.852$ Mg m^{-3}, μ 0.191 mm^{-1}, *F* (000) 768, crystal size $0.50 \times 0.22 \times 0.14$ mm^3, θ range for data collection 3.39 to 29.37°, Ind. reflns 3331, Obs. reflns 2634, R_{int} 0.0381, *GoF* 1.043, R_1 [I > 2σ(I)] 0.0356, wR_2 (all data) 0.0803, largest diff. peak and hole 0.274 and −0.245 e. Å^{-3}.

2.4 Sensitiveness

Sensitiveness data were measured in accordance with established protocols [18]. Sensitiveness to friction was measured using a Julius Peters BAM (German Federal Institute for Testing Materials) friction apparatus (Berlin, Germany). The values reported are the lowest setting at which the 10 mg samples initiated; six repetitions of the experiment at the next lower setting produced nil initiations. Sensitiveness to impact was measured using a Rotter Impact apparatus (Defence Science and Technology Group, Edinburgh, Australia). The experiment was repeated 50 times utilizing 30 mg samples with a standard drop weight of 2 kg and reported values [Figure of Insensitiveness (F of I)] standardized to cyclotrimethylene trinitramine (RDX) (F of I = 80) [19]. Sensitiveness to elevated temperatures [Temperature of Ignition (T of I)] was determined utilizing 50 mg samples (unless stated otherwise) heated (in duplicate) at 5 °C min^{-1} to decomposition within a shielded heating block. Sensitiveness to electrostatic discharges (ESD) was measured by passing electrical discharges of 4.5, 0.45 and 0.045 J through 10 mg samples utilizing equipment purpose built by the Defence Science and Technology Group. The figure reported is the lowest setting at which the samples ignited. Differential Scanning Calorimetry (DSC) was conducted with a TA Instruments (New Castle, Pennsylvania, USA) DSCQ10 scanning from 20 °C to 250 °C at 10 °C min^{-1} under nitrogen using open aluminium pans. Sample size was iteratively increased from 1 mg to the reported 9.4 mg to minimize the possibility of damage to the equipment.

2.5 Theoretical Methods

The molecular structure derived from X-ray crystal analysis was optimized in its singlet and triplet states by the Becke 3LYP method and 6-31 + G(d,p) basis set using the Gaussian 03 program [20–23]. Stationary points were characterized as minima (no imaginary frequencies) by calculation of the frequencies using analytical gradient procedures. The global minimum was then probed using the CBS-4M (complete basis set) method, which is based on the theoretical extrapolation of the basis set to an infinite limit (to completion) [11]. The enthalpy (H) from the CBS calculation was then used to predict the gas phase heat of formation of XPN using the atomisation method; subsequent conversion

to the condensed phase was done by applying Trouton's rule using the melting point as measured by DSC [12, 24–28]. Crystal density, from X-ray crystallographic analysis, and the calculated solid phase heat of formation were inputted to the Cheetah 7.0 program suite to predict detonation parameters [13]. Cheetah is a physics- and chemistry-based tool that employs thermochemical computer code to predict detonation characteristics.

3 Results and Discussion

3.1 Crystal Structure

Rod-shaped crystals of XPN suitable for X-ray diffraction were grown by slow evaporation from a concentrated solution of the compound in ethanol and water. XPN crystallises in the centrosymmetric monoclinic space group $P2_1/n$ with a single molecule in the asymmetric unit (Figure 2).

The density of XPN calculated from the crystal structure is 1.852 g cm^{-3} at 150 K, which is very close to the value reported for ETN (1.851 g cm^{-3} at 140 K [29]) and for PETN (1.845 g cm^{-3} at 100 K [30]). As can be seen from Table 1, the carbon-carbon bond angles for XPN indicate that bonds are more distorted than those in PETN but less distorted than those in ETN. For O—C bonds, distortion in XPN is slightly lower than ETN but significantly higher than PETN.

Close analysis of the crystal structure (Figure 2b) indicates that weak intermolecular hydrogen bonding (CH⋯O) and NO— —ON and NO— —N interactions govern crystal packing (Table 2). All but one of the hydrogen atoms are involved in intermolecular CH⋯O hydrogen bonding with parameters as shown in Table 2.

3.2 Sensitiveness Testing

Sensitiveness testing data for XPN are included in Table 3, along with previously reported results for PETN, RDX and lead azide [18, 31, 32]. For comparison, Table 3 also includes sensitiveness data for ETN, measured at the Defence Science and Technology Group explosive testing facility [33]. It should be noted that while a universally accepted classification system to distinguish primary from secondary explosives is yet to be realised, species that are more sensitive to initiating stimuli than PETN may be considered primary explosives, whereas those less sensitive, as secondary explosives. Lead azide is generally considered a sensitive primary explosive [19].

A 50 mg sample of XPN, heated during a T of I experiment at 5 °C min^{-1} [from an initial temperature of 20 °C], did not noticeably evolve vapour or undergo an energetic event before the experiment was terminated at 250 °C. Upon cooling and subsequent inspection of the sample, the originally white crystalline solid had decomposed to form a dark viscous liquid. To examine if a more vigorous decom-

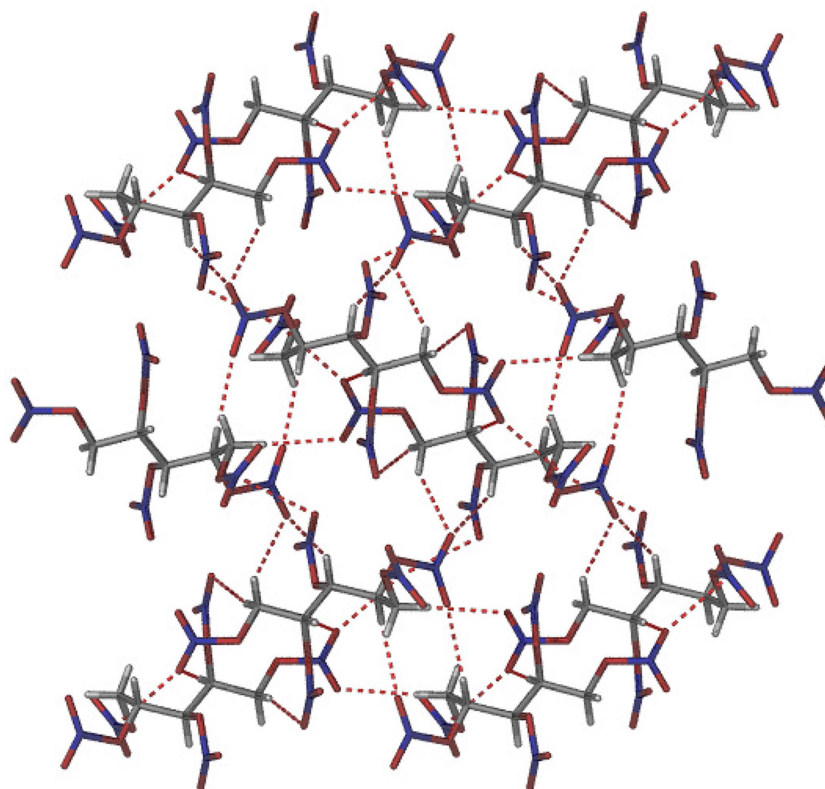**These are not the final page numbers!** ⌐⌐

(a)
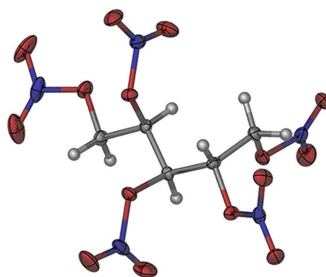
(b)

Figure 2. (a) A representation of the structure of XPN with ellipsoids presented with 50 % probability level. (b) The packing of XPN viewed down the *a*-axis with the weak CH···O hydrogen bonds and NO···N interactions shown with dashed red bonds. Carbon – grey; hydrogen – white; nitrogen – blue; and oxygen – red.

position reaction was observable at a larger scale, the T of I experiment was repeated in duplicate using 100 mg samples. At the increased scale, an evolution of a dark vapour began at 163 °C and was accompanied by an explosive "cracking" sound at 167 °C, typical of a low-moderate energetic/explosive event. This is consistent with the DSC results whereby a 9.4 mg sample heated at 10 °C min^{-1}, having melted at 45.5 °C, exhibited an exothermic decomposition beginning at 169.4 °C, reached a peak maximum at 185.8 °C, and evolved 353 J g^{-1} (see Figure 3). The exotherm is consistent with prior published DSC results of

[10], however herein the full DSC trace, including the melt at 45.5 °C, is reported for the first time. Under similar experimental (DSC) conditions, RDX and lead azide underwent more vigorous exotherms, evolving 2100 and 1298 J g^{-1}, respectively, whereas PETN and ETN produced 240 and 167 J g^{-1}, respectively [34–36].

Comparison of the T of I points of XPN, ETN, PETN and lead azide show XPN to be significantly more sensitive to elevated temperatures compared to lead azide, and similarly sensitive compared to ETN and PETN [18,19,31,32]. It should be noted, however, that the T of I and DSC experi-

Table 1. Comparison of Bond Lengths (Å) and Angles (°) for XPN, ETN and PETN.

BOND	BOND LENGTH RANGE (Å)		
	XPN	ETN[a]	PETN[b]
C—C	1.5135(18)–1.5275(18)	1.5142(16)–1.541(2)	1.53169(13)
C—O	1.4456(17)–1.4542(15)	1.4466(14)–1.4481(14)	1.44634(18)
O_2N—O	1.3977(16)–1.4417(15)	1.3968(13)–1.4246(13)	1.40088(17)
O_2N	1.1923(15)–1.2062(15)	1.1902(13)–1.2080(14)	1.19941(19), 1.2057(2)
	BOND ANGLE RANGE (°)		
C—C—C	111.53(11)–114.97(11)	114.10(12)–114.16(12)	107.998(5), 112.46(1)
C—O—N	112.88(10)–115.52(10)	113.04(9)–114.54(8)	112.95(1)
O—C—C	103.27(10)–108.60(10)	102.37(11)–104.38(9)	106.774(8)
NO_2	129.74(12)–130.82(14)	129.30(11)–130.35(11)	129.53(2)
O_2N—O	111.33(13)–118.10(11)	111.33(9)–118.59(9)	118.01(1), 112.46(1)

[a] Reference 29; [b] Reference 30

Table 2. Weak intermolecular interactions in the crystal packing of XPN.

INTERACTION	D—A DISTANCE (Å)	D—H⋯A ANGLE (°)
C1—H1B⋯O24	3.550	177.32
C2—H2⋯O12	3.309	137.49
C3—H3⋯O113	3.451	145.47
C4—H4⋯O25	3.502	175.85
C5—H5 A⋯O13	3.360	147.79
C5—H5B⋯O20	3.475	163.28
O16⋯N7	2.857	
O25⋯N7	2.758	

Table 3. Sensitiveness Data for XPN, ETN, PETN, Lead Azide and RDX.

	T of I (°C)	F of I (evolved gas, mL)	Friction (N)	ESD (J)
XPN	167	25(6)	18	4.5
ETN	173	40(11)	40	4.5
PETN	181	50(6)	42	0.45
Lead Azide[a]	330	30	5	<0.02
RDX	220	80(12)	80	4.5

[a] T of I, F of I and ESD taken from reference [18], Friction Sensitiveness data from reference [31].

ments should not be viewed as exhaustive analyses of the hazards associated with XPN at elevated temperatures. It remains possible that a change in experimental conditions, such as the heating regime or scale of the experiment, may lead to significantly different results.

Rotter Impact analysis of XPN produced an F of I of 25 (standardized to RDX, F of I = 80, Table 3) from 50 repetitions of the experiment with an average gas evolution of 6 mL. This is significantly more sensitive than PETN (40) and similarly impact sensitive compared to lead azide (30), indicative of a primary explosive [31,32]. Intuitively, the volume of gas evolved from an energetic event may be diagnostic of the performance of an explosive [32]. An average gas evolution of 6 mL for XPN is consistent with a moder-

ate- to high-performance explosive and is similar to that observed for PETN.

Bam friction testing showed that XPN consistently initiated producing a low report (faint cracking sound) when 18 N of frictional force was applied to 10 mg (approximately) samples (Table 3). The explosive did not initiate when subjected to 16 N of frictional force. This is more sensitive than PETN (42 N) and ETN (40 N), but not as sensitive as lead azide (5 N), which is highly susceptible to ignition by frictional stimuli [31,32]. As with Rotter Impact analysis, BAM friction results depict XPN as a primary explosive.

ESD measurements showed that XPN samples repeatedly initiated upon application of 4.5 J, but failed to initiate at 0.45 J. Likewise, the minimum points at which ETN and RDX initiated due to electrical discharges are also in the range of 4.5–0.45 J, typical of insensitive energetic materials or secondary explosives (Table 3) [31,32]. PETN was more sensitive, initiating at between 0.45 and 0.045 J.

In summary, on the basis of the sensitiveness data, XPN may be classified as a primary explosive. While it displayed similar test results during T of I experiments when compared to the PETN and ETN, and was insensitive to electrical discharge, XPN is significantly more sensitive to impact and frictional stimuli compared to PETN.

3.3 Computational Results

The molecular structure determined by X-ray crystallography was used as the input geometry for both the B3LYP/6-31 + G(d,p) and CBS-4M calculations. For completeness, density functional calculations were conducted on singlet and triplet states of XPN. The singlet state (point group = C_1; dipole moment = 0.86 D) was 289.1 kJ mol^{-1} lower in energy than the triplet state (point group = C_1; dipole moment = 0.57 D) and hence the latter species has not been considered further. The optimized structure of the lowest energy conformation calculated [B3LYP/6-31 + G(d,p)] is included in Table 4. For comparison, Table 4 also includes the
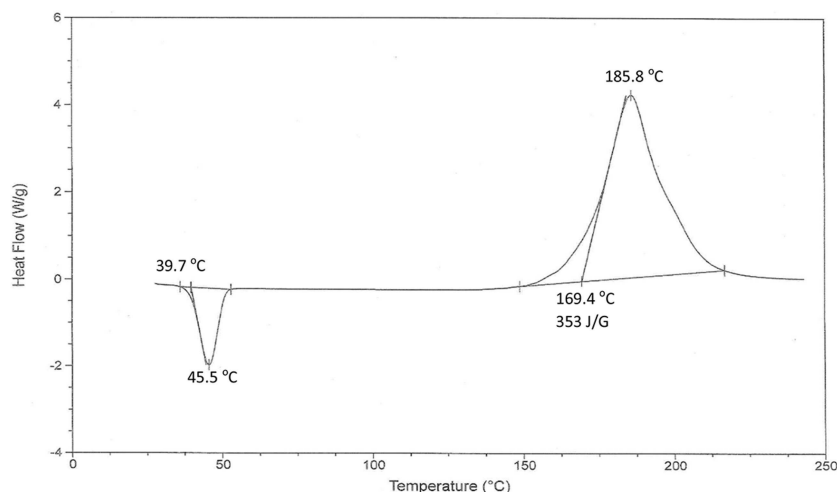
These are not the final page numbers! ↗↗

Figure 3. DSC curve of XPN measured at a heating rate of $10\,°C\,min^{-1}$ under nitrogen.

key bond lengths, bond angles and dihedral angles for XPN derived from X-ray analysis and complete basis set calculation (CBS-4M).

As seen in Table 4, the calculated bond lengths and angles for the B3LYP and CBS-4M calculations were in good agreement with the single crystal X-ray structure. For example, bond lengths C_1C_2 were 1.514 Å, 1.527 Å and 1.514 Å for X-ray, B3LYP and CBS-4M results, respectively. Likewise, bond lengths for C_4O_{12} were 1.450 Å, 1.446 Å and 1.475 Å and N_3O_8 were 1.193 Å, 1.200 Å and 1.204 Å. Bond angles were likewise in good agreement, for example $C_3O_9N_3$ were 115.5° (X-ray), 115.7° (B3LYP) and 114.2° (CBS-4M), whereas $O_{12}N_4O_{10}$ were 117.8°, 117.7° and 116.2° and $C_5O_{13}N_5$ were 113.8°, 113.8° and 113.3°.

As with the bond lengths and angles depicted in Table 4, the experimental and computational dihedral angles were generally in good agreement. For example, dihedral $C_1C_2C_3C_4$ were 53.1° (X-ray), 54.8° (B3LYP) and 54.7° (CBS-4M) and $C_1O_3N_1O_2$ were −1.0°, −1.6° and −2.5°. However, the $C_3O_9N_3O_7$ and $C_3O_9N_3O_8$ dihedral angles for the X-ray results depict this part of the molecular as almost planar, whereas the computational results skew the NO_2 group by approximately 10° (B3LYP) and 20° (CBS-4M). A similar phenomenon, albeit less pronounced, was observed for $C_4O_{12}N_4O_{10}$ and $C_4O_{12}N_4O_{11}$.

The enthalpy ($H^{298} = 1594.360004$ a.u.) from the CBS calculation and the DSC data were used to derive the solid phase heat of formation ($\Delta_f H^0_{(s, Molecule)} = -500.48\,kJ\,mol^{-1}$); see Theoretical Methods section for details. The heat of formation was inputted into the Cheetah 7.0 program suite, with the calculated crystal density ($1.852\,g\,cm^{-3}$) derived from the measured crystal structure, to calculate explosive parameters for XPN (Table 5). For comparison, Table 5 also includes calculated (Cheetah) and experimental literature detonation parameters for ETN, PETN and RDX [30, 37–41].

The calculated (Cheetah) detonation velocity of XPN, $8.780\,km\,s^{-1}$, and detonation pressure, 32.6 GPa, are in good agreement with the entirely computationally derived predictions of Wang *et al.* of $8.610\,km\,s^{-1}$ and 32.3 GPa (Table 5) [6]. The detonation velocity is also comparable to the values calculated for ETN ($8.706\,km\,s^{-1}$), RDX ($8.727\,km\,s^{-1}$) and PETN ($8.843\,km\,s^{-1}$). The Chapman-Jouguet (CJ) pressures were similar for the four explosives. Superficially, XPN displays similar detonation characteristics to the experimental and theoretical data reported for RDX. However, the crystal density of RDX at $1.816\,g\,cm^{-3}$ is close to the charge packing density achieved for this explosive during experimentation (Table 5), and hence the calculated theoretical detonation velocity and pressure are similar to those measured experimentally. This is not the case for ETN, which has a theoretical detonation velocity of $8.706\,km\,s^{-1}$ and a measured value of $8.030\,km\,s^{-1}$ reported for a pressed charge [37]. The detonation velocity for melt cast ETN was similar to that of the pressed material [40]. It may be that further experimentation will narrow the gap between experiment and theory for ETN, however it is also possible that a significantly higher detonation velocity (e.g. $> 8.500\,km\,s^{-1}$) may be impractical due to the sensitivity of the explosive, i.e. it may be too sensitive to sustain significantly greater pressing loads. If this is the case, then it is probable that future experimentally derived explosive performance data for XPN, a significantly more sensitive explosive than ETN, may never approach the maximum theoretical values reported herein.

4 Conclusion

The explosive XPN has been synthesized following a literature procedure and slowly re-crystallized from ethanol and water to produce a crystalline material suitable for single

Table 4. The experimental (X-ray) and calculated (B3LYP/6-31+(d,p) and CBS-4M) structures of XPN.

| Bond Length (Å)	X-ray	B3LYP	CBS-4M	Bond Angle (°)	X-ray	B3LYP	CBS-4M
C_1C_2	1.514	1.527	1.514	$C_5O_{13}N_5$	113.8	113.8	113.3
C_2C_3	1.527	1.542	1.520	$O_{13}N_5O_{14}$	117.7	116.9	116.0
C_3C_4	1.525	1.534	1.514	$O_{13}N_5O_{15}$	112.1	112.5	114.1
C_4C_5	1.515	1.527	1.511	*Dihedral Angle (°)*			
C_1O_3	1.447	1.444	1.471	$C_1C_2C_3C_4$	53.1	54.8	54.7
O_3N_1	1.406	1.435	1.411	$C_2C_3C_4C_5$	−179.3	174.8	162.0
N_1O_1	1.200	1.203	1.212	$C_3C_2C_1O_3$	48.0	45.6	40.9
N_1O_2	1.199	1.212	1.231	$C_2C_1O_3N_1$	177.8	173.2	174.2
C_2O_6	1.454	1.445	1.469	$C_1O_3N_1O_1$	179.4	178.4	177.4
O_6N_2	1.417	1.444	1.413	$C_1O_3N_1O_2$	−1.0	−1.6	−2.5
N_2O_4	1.199	1.200	1.207	$C_4C_3C_2O_6$	173.5	176.0	172.6
N_2O_5	1.206	1.212	1.241	$C_3C_2O_6N_2$	154.4	146.9	157.9
C_3O_9	1.446	1.439	1.469	$C_2O_6N_2O_4$	175.0	−177.0	−173.9
O_9N_3	1.442	1.460	1.422	$C_2O_6N_2O_5$	−4.0	3.6	6.9
N_3O_7	1.196	1.208	1.240	$C_1C_2C_3O_9$	170.1	175.0	173.0
N_3O_8	1.193	1.200	1.204	$C_2C_3O_9N_3$	105.0	108.0	118.9
C_4O_{12}	1.450	1.446	1.475	$C_3O_9N_3O_7$	1.3	11.5	20.8
$O_{12}N_4$	1.441	1.452	1.425	$C_3O_9N_3O_8$	−179.2	−170.0	−161.2
N_4O_{10}	1.193	1.211	1.241	$C_2C_3C_4O_{12}$	62.4	54.9	45.2
N_4O_{11}	1.192	1.200	1.202	$C_3C_4O_{12}N_4$	−141.9	−134.7	−140.8
C_5O_{13}	1.445	1.441	1.466	$C_4O_{12}N_4O_{10}$	18.9	14.3	34.7
$O_{13}N_5$	1.398	1.432	1.410	$C_4O_{12}N_4O_{11}$	−163.4	−167.6	−148.3
N_5O_{14}	1.196	1.213	1.234	$C_3C_4C_5O_{13}$	−192.2	170.7	173.9
N_5O_{15}	1.203	1.203	1.211	$C_4C_5O_{13}N_5$	167.0	175.0	175.3
Bond Angle (°)				$C_5O_{13}N_5O_{14}$	1.6	2.1	2.0
$C_1C_2C_3$	115.0	115.3	113.4	$C_5O_{13}N_5O_{15}$	−178.9	−178.3	−178.3
$C_2C_3C_4$	113.0	114.0	113.1				
$C_3C_4C_5$	111.5	111.5	112.8				
$C_2C_1O_3$	105.5	106.5	104.0				
$C_1O_3N_1$	112.9	114.1	113.6				
$O_3N_1O_1$	112.3	112.3	113.8				
$O_3N_1O_2$	117.8	116.9	116.1				
$C_3C_2O_6$	103.3	103.6	101.5				
$C_2O_6N_2$	114.2	115.1	113.9				
$O_6N_2O_4$	112.2	111.9	114.1				
$O_6N_2O_5$	118.1	117.4	116.2				
$C_4C_3O_9$	106.4	108.6	109.0				
$C_3O_9N_3$	115.5	115.7	114.2				
$O_9N_3O_7$	117.8	117.7	116.4				
$O_9N_3O_8$	111.3	111.2	113.8				
$C_5C_4O_{12}$	108.6	108.8	106.8				
$C_4O_{12}N_4$	115.3	116.0	113.9				
$O_{12}N_4O_{10}$	117.8	117.7	116.2				
$O_{12}N_4O_{11}$	111.6	111.6	114.0				
$C_4C_5O_{13}$	103.7	104.8	102.3				
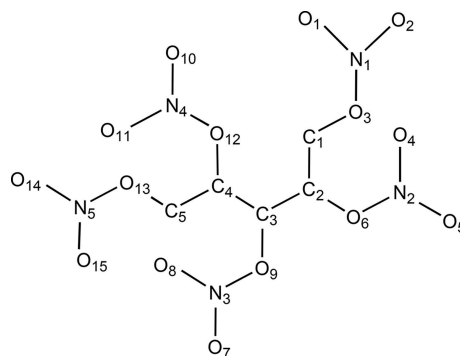
Table 5. Computational and Experimental Parameters for XPN, ETN, PETN and RDX.

	XPN Cal.[a]	Cal. [6]	ETN Cal.[b]	Exp. [39]	PETN Cal.[b]	Exp. [40]	RDX Cal.[b]	Exp. [40]
Density (g cm⁻³)	*1.852*	1.750	1.827 [38]	1.740	1.845 [30]	1.770	1.816 [41]	1.800
Detonation Pressure (GPa)	*32.6*	32.3	31.6	(c)	33.8	33.3	33.6	34.7
Detonation Velocity (km s⁻¹)	*8.780*	8.610	8.706	8.030	8.843	8.500	8.727	8.800

[a] Results from this study; [b] Heat of formation data for calculation taken from [37]; [c] Data not available.

crystal X-ray diffraction and sensitiveness analyses. The crystal forms a close-packed structure sustained by weak intermolecular packing constraints and has a density of 1.852 g cm⁻³ at 150 K. XPN is more sensitive to impact and

frictional stimuli than ETN and PETN and is classified as a primary explosive. The calculated theoretical explosive performance of XPN is similar to predicted detonation characteristics of ETN, PETN and RDX. Due to the sensitivity of XPN, it may be challenging to realise the predicted performance by experimentation.

Acknowledgments

References

[1] I. G. Wright, L. D. Hayward, The Pentitol Pentanitrates, *Can. J. Chem.* **1960**, *38*, 316.

[2] L. D. Hayward, I. G. Wright, Xylitol Pentanitrate Preparation and Denitration, in: *Methods Carbohydr. Chem.* (Eds.: R. L. Whistler, M. L. Wolfrom, J. N. BeMiller) Academic Press Inc., New York, **1963**, p. 258.

[3] S. W. Blum, J. B. Quinn, B. B. Howe, M. A. Hefner, M. M. Winbury, Pharmacologic and Biochemical Evaluation of Organic Nitrates: Attempted Correlation of Activities, *J. Pharmacol. Exp. Ther.* **1971**, *176*, 684.

[4] J. Šarlauskas, K. Krikštopaitis, V. Miliukienė, Z. Anusevičius, A. Šaikūnas, N. Čėnas, Organic Nitrates and Nitramines: Synthesis, electrochemistry and Cyctotoxicity, *New Trends Res. Energ. Mater.* **2010**, Proc. Semin., Czech Republic.

[5] J. Šarlauskas, K. Krikštopaitis, V. Miliukienė, Z. Anusevičius, A. Šaikūnas, N. Čėnas, Investigation on the Electrochemistry and Cytotoxicity of Organic Nitrates and Nitroamines, *Cent. Eur. J. Energ. Mater.* **2011**, *8*, 15.

[6] G. Wang, X. Gong, H. Du, Y. Liu, H. Xiao, Theoretical Prediction of Properties of Aliphatic Polynitrates, *J. Phys. Chem. A,* **2011**, *115*, 795.

[7] M. J. Kamlet, S. J. Jacobs, Chemistry of Detonations. I. A Simple Method for Calculating Detonation Properties of C—H—N—O Explosives, *J. Chem. Phys.* **1968**, *48*, 23.

[8] X. Zhang, H. Xiao, Computational Studies on the Infrared Vibrational Spectra, Thermodynamic Properties, Detonation Properties, and Pyrolysis Mechanism of Octanitrocubane, *J. Chem. Phys.* **2002**, *116*, 10674.

[9] Y. Qi-Long. M. Künzel, S. Zeman, R. Svoboda, M. Bartošková, The Effect of Molecular Structure on Thermal Stability, Decomposition Kinetics and Reaction models of Nitric Esters, *Thermochim. Acta* **2013**, *566*, 137.

[10] J. Dong, Y. Qi-Long, L. Pei-Jin, H. Wei, X. Qi, S. Zeman, The Correlations Among Detonation Velocity, Heat of Combustion, Thermal Stability and Decomposition Kinetics of Nitric Esters, *J. Therm. Anal. Calorim.* **2018**, *131*, 1391.

[11] J. A. Montgomery, M. J. Frisch, J. W. Ochterski, G. A. Petersson, A Complete Basis Set Model Chemistry. VII. Use of the Minimum Population Method, *J. Chem. Phys.* **2000**, *112*, 6532.

[12] T. M. Klamotke, *Chemistry of High-Energy Materials 2nd Edition*, Walter de Gruyter GmbH & Co. KG, Berlin **2012**, p. 89.

[13] Cheetah 7.0, Energetic Materials Center, Lawrence Livermore National Laboratory.

[14] CrysAlisPro, CrysAlis171.NET, Verson 1.171.34.44, Oxford Diffraction Ltd: Oxfordshire, U.K., **2010**.

[15] G. M. Sheldrick, Phase Annealing in SHELX-90: Direct Methods for Large Structures. *Acta Crystallogr. Sect. A* **1990**, *46*, 467.

[16] G. M. Sheldrick, SHELXL-2014, University of Göttingen, Göttingen, Germany, **2014**.

[17] L. J. Barbour, X-Seed – A Software Tool for Supramolecular Crystallography, *J. Supramol. Chem.* **2001**, *1*, 189.

[18] Energetic Materials Testing and Assessment Policy Committee. Manual of Tests, Issue One, United Kingdom Ministry of Defence, U.K., **2002**.

[19] M. E. Smith, C. Wall, M. Fitzgerald, Characterisation of the Major Synthetic Products of the Reactions Between Butanone and Hydrogen Peroxide, *Propellants Explos. Pyrotech.* **2012**, *37*, 282.

[20] A. D. Becke, Density-functional Thermochemistry. III. The Role of Exact Exchange, *J. Chem. Phys.* **1993**, *98*, 5648.

[21] P. J. Stevens, F. J. Devlin, C. F. Chablowski, M. J. Frische, *J. Phys. Chem.* **1994**, *98*, 11623.

[22] a) T. H. Dunning, Gaussian Basis Sets For Use in Correlated Molecular Calculations. I. The Atoms Boron Through Neon and Hydrogen, *J. Chem. Phys.* **1989**, *90*, 1007; b) D. E. Woon, T. H. Dunning, Gaussian Basis Sets for Use in Correlated Molecular Calculations. III. The Atoms Aluminum Through Argon, *J. Chem. Phys.* **1993**, *98*, 1358; c) T. H. Dunning, K. A. Peterson, D. E. Woon, Basis Sets: Correlation Consistent, in *Encyclopedia of Computational Chemistry*, (Eds.: P. V. R. Schleyer), Wiley: Chichester, UK, **1998**.

[23] M. J. Frisch, G. W. Trucks, H. B. Schlegel, G. E. Scuseria, M. A. Robb, J. R. Cheeseman, J. A. Montgomery Jr, T. Vreven, K. N. Kudin, J. C. Burant, J. M. Millam, S. S. Iyengar, J. Tomasi, V. Barone, B. Mennucci, M. Cossi, G. Scalmani, N. Rega, G. A. Petersson, H. Nakatsuji, M. Hada, M. Ehara, K. Toyota, R. Fukuda, J. Hasegawa, M. Ishida, T. Nakajima, Y. Honda, O. Kitao, H. Nakai, M. Klene, X. Li, J. E. Knox, H. P. Hratchian, J. B. Cross, V. Bakken, C. Adamo, J. Jaramillo, R. Gomperts, R. E. Stratmann, O. Yazyev, A. J. Austin, R. Cammi, C. Pomelli, J. W. Ochterski, P. Y. Ayala, K. Morokuma, G. A. Voth, P. Salvador, J. J. Dannenberg, V. G. Zakrzewski, S. Dapprich, A. D. Daniels, M. C. Strain, O. Farkas, D. K. Malick, A. D. Rabuck, K. Raghavachari, J. B. Foresman, J. V. Ortiz, Q. Cui, A. G. Baboul, S. Clifford, J. Cioslowski, B. B. Stefanov, G. Lui, A. Liashenko, P. Piskorz, I. Komaromi, R. L. Martin, D. J. Fox, T. Keith, M. A. Al-Laham, C. Y. Peng, A. Nanayakkara, M. Challacombe, P. M. W. Will, B. Johnson, W. Chen, M. W. Wong, C. Gonzalez, J. A. Pople, GAUSSIAN 03; Gaussian, Inc., Wallingford CT, **2004**.

[24] P. Politzer, J. S. Murray, M. E. Grice, M. Desalvo, E. Miller, Calculation of Heats of Sublimation and Solid Phase Heats of Formation, *Mol. Phys.* **1997**, *91*, 923.

[25] L. A. Curtiss, K. Raghavachari, P. C. Redfern, J. A. Pople, Assessment of Gaussian-2 and Density Functional Theories for the Computation of Enthalpies of Formation, *J. Chem. Phys.* **1997**, *106*, 1063.

[26] E. F. C. Byrd, B. M. Rice, Improved Prediction of Heats of Formation of Energetic Materials Using Quantum Mechanical Calculations, *J. Phys. Chem. A.* **2006**, *110*, 1005.

[27] B. M. Rice, S. V. Pai, J. Hare, Predicting Heats of Formation of Energetic Materials Using Quantum Mechanical Calculations, *Combust. Flame* **1999**, *118*, 445.

↖↖ **These are not the final page numbers!**

[28] M. S. Westwell, M. S. Searle, D. J. Wales, D. H. Williams, Empirical Correlations between Thermodynamic Properties and Intermolecular Forces, *J. Am. Chem. Soc.* **1995**, *117*, 5013.

[29] V. W. Manner, B. C. Tappan, B. L. Scott, D. N. Preston, G. W. Brown, Crystal Structure, Packing Analysis, and Structural-Sensitivity Correlations of Erythritol Tetranitrate, *Cryst. Growth Des.* **2014**, *14*, 6154–6160.

[30] E. A. Zhurova, A. I. Stash, V. G. Tsirelson, V. V. Zhurov, E. V. Bartashevich, V. A., Potemkin, A. A. Pinkerton, Atoms-in-molecules study of intra-and intermolecular bonding in the pentaerythritol tetranitrate crystal, *J. Am. Chem. Soc.* **2006**, *128*, 14728–14734

[31] C. Bulian, L. Thompson, H. S. Lee, Determination of Lead Azide Arrhenius Kinetics Constants, *49th AIAA* **2011**, 1.

[32] M. Fitzgerald, M. G. Gardiner, D. Armitt, G. W. Dicinoski, C. Wall, Confirmation of the Molecular Structure of Tetramethylene Diperoxide Dicarbamide (TMDD) and Its Sensitiveness Properties, *J. Phys. Chem. A* **2015**, *119*, 905.

[33] Unreported study conducted on ETN at the Defence Science and Technology Group, Edinburgh, Australia.

[34] S. Mathew, K. Krishnan, K. N. Ninan, A DSC Study on the Effect of RDX and HMX on the Thermal Decomposition of Phase Stabilized Ammonium Nitrate, *Propellants Explos. Pyrotech.* **1998**, *23*, 150.

[35] L. Thompson, A. Konst, H. S. Lee, Preliminary Investigation of SPLA/RD-1333 Lead Azide Thermal Decomposition Kinetics. *48th AIAA* **2010**, 1.

[36] M. Künzel, Q. Yan, J. Šelešovský, S. Zeman, R. Matyáš, Thermal Behaviour and Decomposition Kinetics of ETN and its Mixtures with PETN and RDX, *J. Therm. Anal. Calorim.* **2014**, *115*, 289.

[37] J. C. Oxley, J. L. Smith, J. E. Brady IV, A. C. Brown, Characterisation and Analysis of Tetranitrate Esters, *Propellants Explos. Pyrotech.* **2012**, *37*, 24.

[38] R. Matyáš, M. Künzel, A. Růžička, P. Knotek, O. Vodochodský, Characterisation of Erythritol Tetranitrate Physical Properties, *Propellants Explos. Pyrotech.* **2015**, *40*, 185.

[39] V. W. Manner, D. N. Preston, B. C. Tappan, V. E. Sanders, G. Brown, E. Hartline, B. Jensen, Explosive Performance Properties of Erythritol Tetranitrate (ETN), *Propellants Explos. Pyrotech.* **2015**, *40*, 460.

[40] S. M. Kaye, *Encyclopaedia of Explosives and Related Items Vol 8–9*, **1980**, US Army Research and Development Command, Dover, New Jersey.

[41] G. R. Miller, A. N. Garroway, A Review of the Crystal Structures of Common Explosives Par I: RDX, HMX, TNT, PETN and Tetryl, Naval Research Laboratory, **2001**, NRL/MR/6120-01-8585.

FULL PAPER
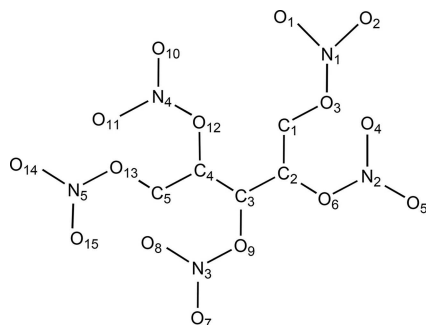
K.-A. S. Stark, J. F. Alvino, K. P. Kirkbride, C. J. Sumby, G. F Metha, C. E. Lenehan, M. Fitzgerald*, C. Wall, M. Mitchell, C. Prior

1 – 10

Crystal Structure, Sensitiveness and Theoretical Explosive Performance of Xylitol Pentanitrate (XPN)